iScience

CellPress
OPEN ACCESS

Article

Inhalation of ACE2 as a therapeutic target on sex-bias differences in SARS-CoV-2 infection and variant of concern

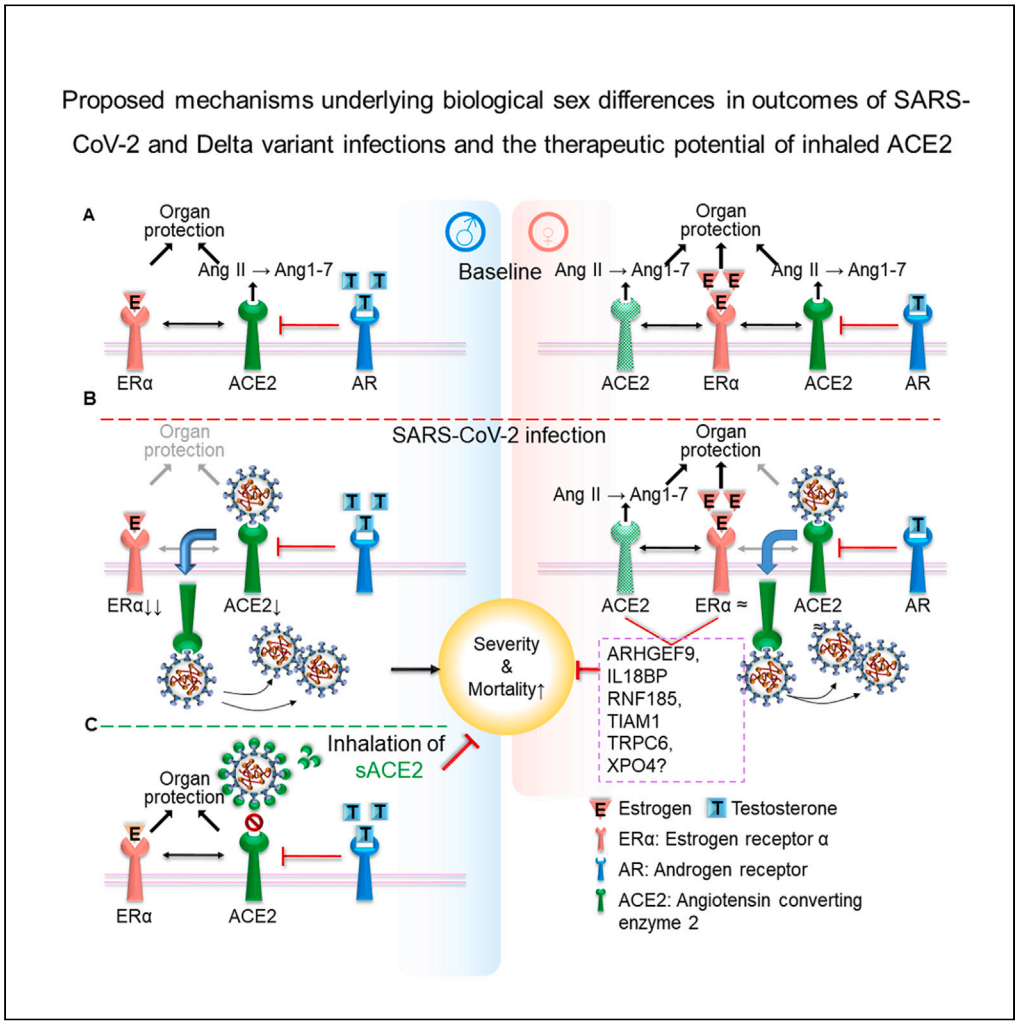

Yu Onodera, Jady Liang, Yuchong Li, ..., Yimin Li, Samira Mubareka, Haibo Zhang

dryiminli@gzhmu.edu.cn (Y.L.)
samira.mubareka@sunnybrook.ca (S.M.)
haibo.zhang@unityhealth.to (H.Z.)

Highlights

K18-hACE2 mice show sex-dependent responses to SARS-CoV-2 infection

Male and female mice display distinct proteomic signatures in SARS-CoV-2 infection

Inhalation of ACE2 reduces SARS-CoV-2 infection via decoy action and ERα modulation

Recombinant ACE2 inhibits Delta variant and cytopathic effects in lung organoids

Onodera et al., iScience 26, 107470
August 18, 2023
https://doi.org/10.1016/j.isci.2023.107470

iScience

CellPress
OPEN ACCESS

Article

Inhalation of ACE2 as a therapeutic target on sex-bias differences in SARS-CoV-2 infection and variant of concern

Yu Onodera,[1,2,17] Jady Liang,[1,3,17] Yuchong Li,[1,4] Bryan Griffin,[5,6] Thenuka Thanabalasingam,[1] Cong Lu,[1] JiaYi Zhu,[1,3] Mingyao Liu,[7] Theo Moraes,[8] Wenhua Zheng,[9] Jasmin Khateeb,[1,10] Julie Khang,[1] Yongbo Huang,[4] Mirjana Jerkic,[1] Masaki Nakane,[2] Andrew Baker,[1,11,12] Beverley Orser,[11] Ya-Wen Chen,[13] Gerald Wirnsberger,[14] Josef M. Penninger,[15,16] Ori D. Rotstein,[1,7] Arthur S. Slutsky,[1,4,12] Yimin Li,[4,*] Samira Mubareka,[5,6,*] and Haibo Zhang[1,3,4,11,12,18,*]

SUMMARY

Despite similar infection rates, COVID-19 has resulted in more deaths in men than women. To understand the underlying mechanisms behind this sex-biased difference in disease severity, we infected K18-human angiotensin converting enzyme 2 (ACE2) mice of both sexes with SARS-CoV-2. Our study revealed a unique protein expression profile in the lung microenvironment of female mice. As a result, they were less vulnerable to severe infection, with higher ACE2 expression and a higher estrogen receptor α (ERα)/androgen receptor (AR) ratio that led to increased antiviral factor levels. In male mice, inhaling recombinant ACE2 neutralized the virus and maintained the ERα/AR ratio, thereby protecting the lungs. Our findings suggest that inhaling recombinant ACE2 could serve as a decoy receptor against SARS-CoV-2 and protect male mice by offsetting ERα-associated protective mechanisms. Additionally, our study supports the potential effectiveness of recombinant ACE2 therapy in human lung organoids infected with the Delta variant.

INTRODUCTION

Males are more likely to be hospitalized, to be admitted to the ICU, and to have a higher mortality rate from COVID-19 than females, across all age groups, except for individuals over 90 years of age.[1–4] This increased mortality is not due to a higher infection rate of males with severe acute respiratory syndrome coronavirus 2 (SARS-CoV-2), as a global meta-analysis of over 3 million COVID-19 cases has shown.[2] Another study of over 38,000 individuals who underwent COVID-19 testing found that 53% of the positive cases were female and 47% were male.[4] The exact cause of these differences is not known, but it may be related to X chromosome-linked signaling pathways or female sex hormones.[5]

Angiotensin converting enzyme 2 (ACE2) plays a major role in the pathogenesis of COVID-19 because of its two main biological functions. It catalyzes the conversion of angiotensin II (Ang II) to angiotensin 1-7 (Ang1-7) for organ protection, and it serves as the host cell receptor for the entry of SARS-CoV-2 into cells.[6] The ACE2 gene is located on the X chromosome, where genes are known to avoid X-inactivation,[7] which contributes to differences between the sexes.[8] The spike proteins of SARS-CoV-2 bind to ACE2,[9] and the expression of ACE2 can be regulated by estrogen receptor-associated signaling pathways[10,11] and by the administration of soluble recombinant ACE2 (rACE2).[12]

We hypothesized that regulation of immune responses by sex hormones and expression of ACE2 are crucial factors in determining sex differences in COVID-19 outcomes. In our study, we investigated the distribution of SARS-CoV-2 in different organs and the progression of clinical manifestation indices in male and female mice expressing human transgene ACE2. We then examined the relationship between 17β-estradiol levels, estrogen receptor α (ERα)/androgen receptor (AR) ratio, and ACE2 expression in the lung tissue of both male and female mice before and after SARS-CoV-2 infection. Our results showed that sex hormone receptor-associated signaling pathways regulated ACE2 expression and

[1]Keenan Research Centre for Biomedical Science, St. Michael's Hospital, Unity Health Toronto, Toronto, ON, Canada

[2]Department of Emergency and Critical Care Medicine, Faculty of Medicine, Yamagata University, Yamagata, Japan

[3]Department of Physiology, University of Toronto, Toronto, ON, Canada

[4]The State Key Laboratory of Respiratory Disease, Guangzhou Institute of Respiratory Disease, The First Affiliated Hospital of Guangzhou Medical University, Guangzhou, China

[5]Department of Laboratory Medicine and Pathobiology, University of Toronto, Toronto, ON, Canada

[6]Department of Medical Microbiology and Infectious Disease, Sunnybrook Health Science Centre, Toronto, ON, Canada

[7]Department of Surgery, University of Toronto, Toronto, ON, Canada

[8]Department of Pediatrics, University of Toronto, Toronto, ON, Canada

[9]Faculty of Health Science, University of Macau, Macau, China

[10]Department of Internal Medicine D, Rambam Health Care Campus, Haifa, Israel

[11]Department of Anesthesiology and Pain Medicine, University of Toronto, Toronto, ON, Canada

[12]Interdepartmental Division of Critical Care Medicine,

Continued

renin-angiotensin system (RAS) pathways, making female mice less susceptible to SARS-CoV-2 infection compared to male mice.

We then explored the microenvironment of ERα-associated signaling pathways in the lung tissue before and after treatment with inhalation of soluble human rACE2 in mice infected with SARS-CoV-2. Our results showed that starting 48 h after SARS-CoV-2 infection, the therapeutic administration of a rACE2 aerosol effectively protected male mice from lung injury through direct neutralization of SARS-CoV-2 and indirect modulation of cellular ACE2 levels and ERα-associated signal pathways. Finally, we validated the relevance of the rACE2 therapy in a human lung organoid model infected with the Delta variant of SARS-CoV-2, supporting the translational potential of this therapeutic intervention approach.

RESULTS

Sex-dependent responses to SARS-CoV-2 infection in the lung of K18-hACE2 mice

To assess the impact of sex on the severity of SARS-CoV-2 infection, male and female keratin 18-human angiotensin converting enzyme 2 (K18-hACE2) mice were infected with the SB2[13] strain of SARS-CoV-2 at a dose of 4×10^5 median tissue culture infectious dose (TCID50). Saline was used as a control. We observed that male mice experienced a marked decline in body weight starting 5 days post-infection (dpi), whereas female mice sustained their weight (Figure 1A). Lung injury scores were higher (Figure 1B) in male mice compared to female mice at 7 dpi. The qPCR analysis revealed that the copy number of the SARS-CoV-2 envelope (E) gene in nasal swab was consistently higher in male mice compared to female mice, indicating that the latter were less susceptible to the virus and were able to clear it more efficiently (Figure 1C). At the same time point, the expression of the E gene (Figure 1D) and the RNA-dependent RNA polymerase (RdRp) gene (Figure 1E) in the lung tissue was higher in male than female mice (Figures 1F and 1G). The expression of the nucleocapsid protein of SARS-CoV-2 was detected in lung tissue of male mice and only minimally in female mice (Figure 1H). The expression of membrane receptor of advanced glycation end-products (RAGE), a specific biomarker of type I alveolar cells[14] in lung tissue, decreased in male mice at 7 dpi (Figure 1I) while plasma levels of cleaved RAGE increased in male mice but not in female mice (Figure 1J). These findings suggest that female mice are less susceptible to the severe consequences of SARS-CoV-2 infection compared to male mice.

ACE2 expression, 17β estradiol levels, and ERα/AR ratio in responses to SARS-CoV-2 infection

The expression of human ACE2 was evaluated and found to be similar in males and females at baseline. However, a dramatic decrease was observed in the expression of human ACE2 in males (Figure 1I). No alterations were observed in the levels of transmembrane serine protease 2 (TMPRSS2) in the lung tissue of either gender. The expression of ERα in the lung tissue was decreased in response to SARS-CoV-2 infection in male mice but remained unchanged in female mice (Figure 1I). Additionally, our observations revealed a robust connection between ERα and cellular ACE2, as demonstrated by a strong linear correlation in protein expression (Figure 1K). There was also a correlation between the expression of ERs and a cluster of proteins including the RAS (Figure S1). The ERα/AR ratio in the lung tissue was found to be significantly lower in male mice compared to female mice both at baseline and after infection (Figures 1I and 1L). The level of 17β estradiol in lung tissue was higher in female mice compared to male mice at baseline and remained higher even after infection, although the difference did not reach statistical significance (Figure 1M). These results suggest that a higher level of 17β estradiol and a greater ERα/AR ratio in female mice may be associated with increased organ protection in response to SARS-CoV-2 infection as compared to male mice.

Male and female mice display different proteomic signatures in response to SARS-CoV-2 infection

We conducted proteomic analyses of lung tissue to assess differences in cell organization, development, DNA and protein metabolism, RNA transcription, and stress responses. At baseline, we found unique expression of proteins in lung tissue between male and female mice. Notably, some proteins expressed only in female mice, and conversely, some proteins, were expressed only in male mice at baseline (Figures 2A, 2B, and S2). Seven dpi, we noticed that six proteins, which were only expressed in female lung tissue, remained present (Figures 2A and 2C). Furthermore, we observed alterations in the expression of proteins linked to the ERα signaling pathway in the lung tissue of both male and female mice, with

University of Toronto, Toronto, ON, Canada

[13]Black Family Stem Cell Institute, Department of Cell, Developmental and Regenerative Biology, Icahn School of Medicine at Mount Sinai, New York city, NY, USA

[14]Apeiron Biologics AG, Campus-Vienna-Biocenter 5, Vienna, Austria

[15]Institute of Molecular Biotechnology of the Austrian Academy of Sciences, Vienna, Austria

[16]Department of Medical Genetics, Life Sciences Institute, University of British Columbia, Vancouver, BC, Canada

[17]These authors contributed equally

[18]Lead contact

*Correspondence: dryiminli@gzhmu.edu.cn (Y.L.), samira.mubareka@sunnybrook.ca (S.M.), haibo.zhang@unityhealth.to (H.Z.)

https://doi.org/10.1016/j.isci.2023.107470

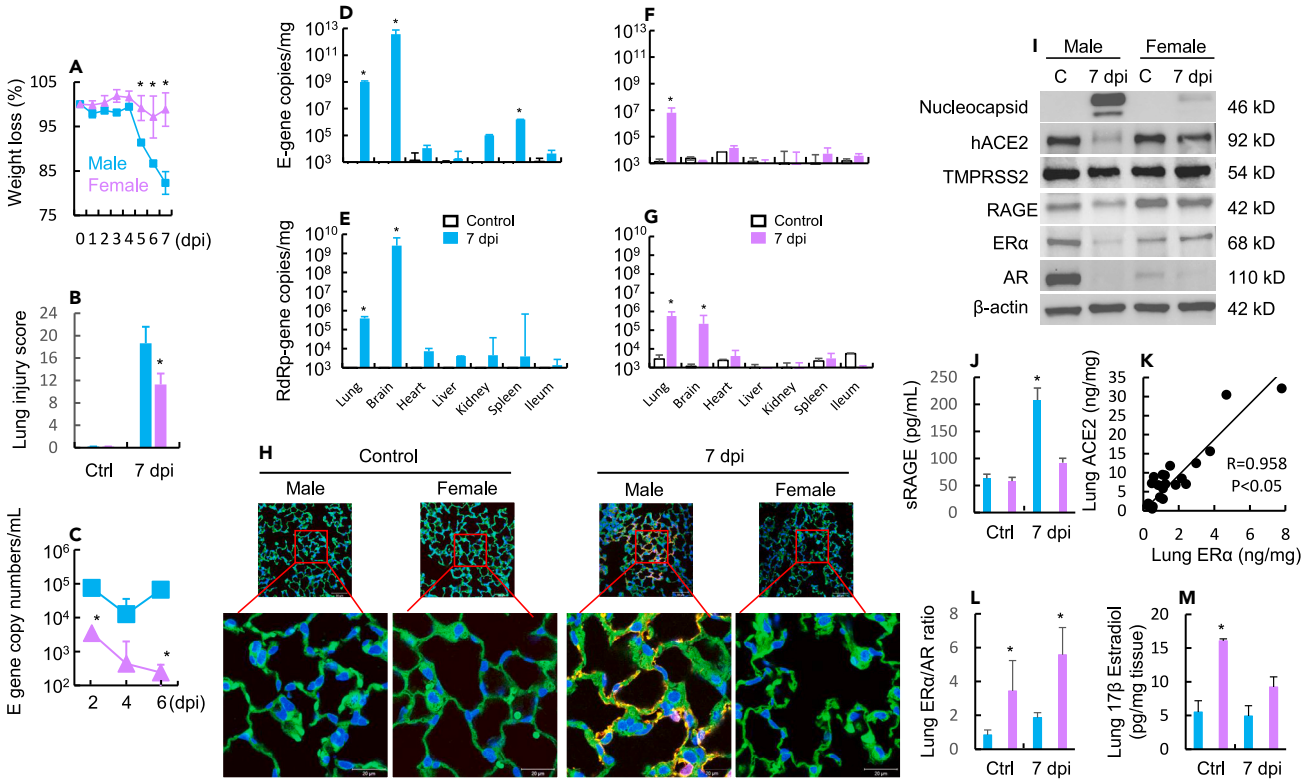

Figure 1. SARS-CoV-2 infection in male and female k18-hace2 mice over 7 days post-infection (dpi)

(A) Body weight loss in response to intranasal inoculation of SARS-CoV-2 (4×10^5 TCID50/50μL/mouse). *$p < 0.05$ vs. male. Data represented in median ± IQR.

(B) Lung injury scoring assessed on a scale of 0–4 for each of the following criteria: 1) neutrophil numbers in the alveolar space, 2) alveolar septal thickening, 3) number of hyaline membranes, 4) alveolar hemorrhage, and 5) cellular hyperplasia. *$p < 0.05$ vs. Ctrl and male. Data represented in mean ± SEM.

(C) Viral RNA levels in oropharyngeal swabs at 2, 4, and 6 dpi. *$p < 0.05$ vs. male. Data represented in median ± IQR.

(D–G) Copy numbers of E-gene and RdRp-gene in multiple organ tissues. *$p < 0.05$ vs. Ctrl. Data represented in mean ± SEM.

(H) Detection of SARS-CoV-2 nucleocapsid protein (red) in lung tissues. Scale bars, 50 μm (main images) and 20 μm (magnified).

(I) Protein expression in lung tissue detected by western blots in vehicle control (C) and at 7 dpi.

(J) Concentration of soluble RAGE protein in plasma in vehicle control and at 7 dpi. *$p < 0.05$ vs. other groups. Data represented in mean ± SEM.

(K) Correlation of protein levels of ACE2 and ERα in lung tissue of male mice before and after infection at 7 dpi.

(L) Estrogen receptor alpha (ERα)/androgen receptor (AR) ratio assessed from western blot analysis in relation to β-actin loading control. *$p < 0.05$ vs. male. Data represented in mean ± SEM.

(M) Concentration of 17β Estradiol in lung tissue homogenates in vehicle control and at 7 dpi. *$p < 0.05$ vs. male. $n = 5$–7 biologically independent mice for all groups. Data represented in mean ± SEM. (see also Figure S1).

discernible variations between the two genders (Figure 2D). These results indicate that the varying baseline conditions lead to sex-specific immune responses to SARS-CoV-2 infection in mice.

Pharmacokinetics of nebulization and intravenous delivery of rACE2

Our results indicated that ACE2 downregulation was less pronounced in female mice after SARS-CoV-2 infection (Figure 1J). To test the protective effects of exogenously administered ACE2, we intravenously delivered clinical grade rACE2 (0.4 mg/kg) using a rabbit model of acute lung injury (ALI). We found that rACE2 metabolic activity was significantly higher in the ALI group and that plasma levels of human ACE2 declined over 6 h after reaching a peak at 1 h (Figures S3A–S3C). These results led us to investigate inhalation delivery of rACE2 to reach the lungs without significant lung injury or at early stages of disease.

We established a nebulization method for delivering rACE2 directly into the lungs and found no degradation of rACE2 during the process (Figure S3D). The antiviral activity of the rACE2 was preserved as shown by the attenuation of SARS-CoV-2 E gene copy numbers in a Vero E6 cells *in vitro* model (Figure S3E).

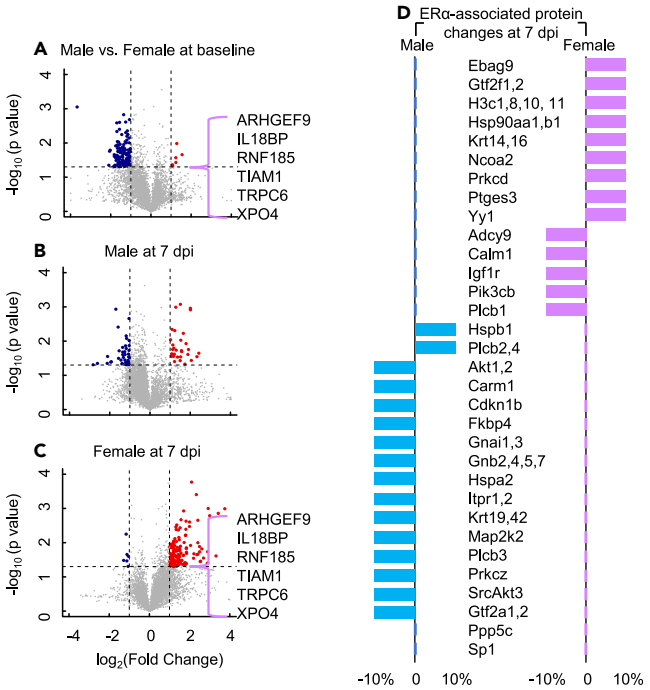

Figure 2. Proteomic profiles in male and female mice at 7 dpi

(A) A volcano plot illustrates significantly different abundant proteins. The -log10 (Benjamini-Hochberg corrected p value) is plotted against the log2 (fold change: female/male) at baseline. (see also Figure S2).

(B and C) Volcano plots illustrate significantly different abundant proteins. The -log10 is plotted against the log2 (fold change: 7 dpi/Ctrl) in male and female mice, respectively. The six unique proteins present in female but not in male mice before and at 7 dpi of SARS-CoV-2 are also shown.

(D) Changes of ERα-associated proteins by at least 10% at 7 dpi compared to control.

Our data prompted us to use an inhalation approach for rACE2 delivery in humanized K18-hACE2 mice. We observed that the aerosol was evenly distributed in the lung, as assessed with Evans Blue delivered via the nebulization system in healthy mice (Figure S3F). We found that human ACE2 levels peaked at 2 h and gradually decreased over 24 h in lung tissue (Figure S3G) while they were 10 times lower and remained unchanged in the plasma (Figure S3H).

To test the dose-dependent response to daily nebulization of rACE2, we conducted a pilot study using K18-hACE2 male mice 48 h after infection with the SARS-CoV-2 strain sunnybrook 2 (SB2)[13] (Figure S3I). We administered either 1.2 mg/kg or 12 mg/kg of rACE2 for 5 days. The results showed that the group treated with 12 mg/kg had an attenuated E gene copy number and a marked reduction in body weight loss (Figures S3J and S3K). However, no such effects were observed in the group treated with 1.2 mg/kg rACE2 (data not shown). Based on these results, we chose the 12 mg/kg dose of rACE2 for subsequent studies.

Inhalation of rACE2 mitigated SARS-CoV-2 infection by modulating ERα signaling

K18-hACE2 male mice were inoculated with SARS-CoV-2,[13] and daily nebulization of rACE2 or vehicle control was begun 48 h after the infection (Figure 3A). At 7 dpi, the levels of E gene and TCID50 in the lung decreased significantly in the rACE2-treated group compared to the vehicle control group (Figures 3B and 3C). Treatment with rACE2 also resulted in a lower expression level of interleukin (IL)-6 (Figure 3D) and decreased plasma soluble RAGE (Figure 3E). The rACE2-treated group showed undetectable expression of the SARS-CoV-2 nucleocapsid protein in the lung as compared to the control group (Figure 3F) and lower lung injury score (Figure 3G). The cellular ACE2 levels in the lung of the rACE2-treated animals were like those of the control animals (Figures 3H and 3I), and the levels of 17β estradiol and the ERα/AR ratio were increased as assessed by ELISA and densitometry, respectively (Figures 3J and 3K).

A potential mechanism behind the protective effects of rACE2 is virus neutralization, which reduces infection and inflammation (Figures S3J and S3K). Our goal in conducting a proteomic analysis of lung tissue was

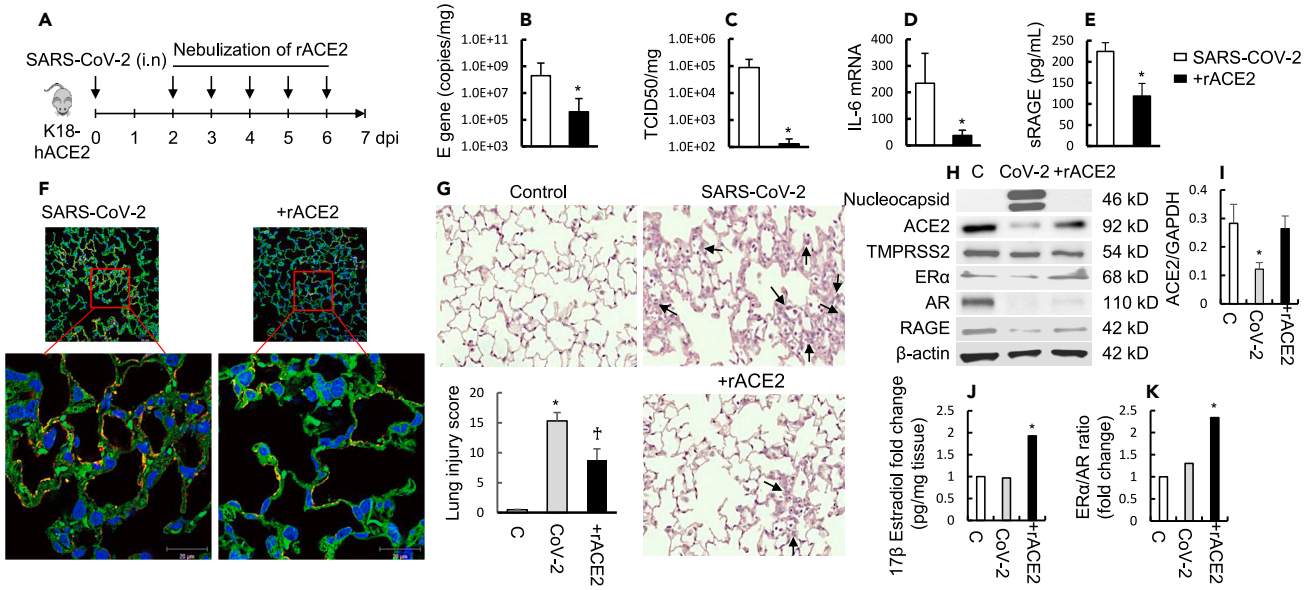

Figure 3. Inhalation of rACE2 attenuates SARS-CoV-2 infection, replication, and lung injury and recovers expression of endogenous ACE2 and ERα in K18-hACE2 male mice at 7 dpi

(A) Study scheme. Mice were intranasally inoculated with SARS-CoV-2 (4×10^5 TCID50/50μL/mouse) and 48 h later received daily nebulization of rACE2 (12 mg/kg) or vehicle control solution for 5 days.

(B and C) Copy numbers of viral envelope (E) gene by RT-qPCR and titers (TCID50) in lung tissue in the SARS-CoV-2 infection alone and rACE2-treated groups. *p < 0.05 vs. SARS-CoV-2. Data represented in mean ± SEM.

(D) Gene expression of IL-6 in lung tissue in the infection alone and rACE2-treated groups. *p < 0.05 vs. SARS-CoV-2. Data represented in mean ± SEM.

(E) Concentration of soluble RAGE protein in plasma in infection alone and rACE2-treated mice. *p < 0.05 vs. SARS-CoV-2. Data represented in mean ± SEM.

(F) Detection of SARS-CoV-2 nucleocapsid protein (red) in lung tissues. Scale bars, 50 μm (main images) and 20 μm (magnified).

(G) Representative lung histology by H&E staining. Arrows indicate neutrophil infiltration in the alveolar space. Lung injury scores from 6 animals per group are also shown. *p < 0.05 vs. naive control (C), ǂp < 0.05 vs. SARS-CoV-2 alone & (C). Data represented in mean ± SEM.

(H and I) Protein expression in lung tissue detected by western blots in naive control (C), SARS-CoV-2 (CoV2) alone, and rACE2-treated groups. *p < 0.05 vs. C & rACE2-treated groups. Data represented in mean ± SEM.

(J and K). Fold changes in the concentrations of 17β Estradiol and ERα/AR ratio assessed from western blot analysis in relation to β-actin loading control in lung tissue in naive control (C), SARS-CoV-2 (CoV2) alone, and rACE2-treated groups. *p < 0.05 vs. C and SARS-CoV-2, respectively. *n* = 5–7 biologically independent mice for all groups. Data represented in mean ± SEM. (see also Figure S3).

to uncover the underlying protective mechanisms. The results, shown in Figure 4, demonstrate a reversal of protein expression in male mice following the administration of rACE2 nebulization during SARS-CoV-2 infection. Intriguingly, the proteins named Really Interesting New Gene Finger Protein 185 (RNF185) and Transient Receptor Potential Cation Channel 6 (TRPC6), previously only detected in female mice before and after SARS-CoV-2 infection, were also present in male lung tissue after treatment with rACE2. Furthermore, our analysis revealed that 31 ERα-associated signaling proteins were upregulated and 10 were downregulated in the lung tissue of the rACE2-treated group. Notably, 16 of these proteins (highlighted in purple, Figures 2A and 2B) were also present in female mice without rACE2 treatment at 7 dpi.

Inhibition of Delta variant replication and cytopathic effects in human lung organoids by human rACE2 protein

We investigated the decoy effects of rACE2 on human lung organoids, which mimic key functions of mature human lung tissue, including expression of pro-surfactant protein C (Pro-SPC) and epithelial cell adhesion molecule (EpCAM) as shown in Figure 5A. Under z stack scanning, we observed robust expression of ACE2 on the surface and inside of control human lung organoids (Figures 5B and S4A). Upon exposure to the Delta variant (1.8×10^7 TCID50/mL), the surface expression of ACE2 decreased in conjunction with increased intracellular expression of viral nucleocapsid protein at 4 h post-infection (hpi) (Figures 5B and S4B). However, when a mixture of Delta variant and rACE2 (400 μg/mL) was applied to the lung organoids for 30 min prior to infection, ACE2 expression was preserved, and there was a marked decrease in the expression of viral nucleocapsid protein at 4 hpi (Figures 5B and S4C). The antiviral effects of rACE2 were tested at doses ranging from 25 to 200 μg/mL, revealing a significant reduction in viral replication at a dose of ≥50 μg/mL and

Figure 4. Nebulization of rACE2 partially restores the ERα-associated signaling proteomic profiles in lung tissue at 7 dpi

Proteomic analysis revealed that treatment with rACE2 resulted in an increase in 31 ERα-associated proteins and a decrease in 10 proteins. Of note, 16 of these proteins (highlighted in purple) were also found in female mice without rACE2 treatment at 7 dpi.

complete suppression of viral progeny of the Delta variant at a dose of ≥25 μg/mL (Figure 5C). Furthermore, rACE2 was found to decrease the cytopathic effects of the virus on human lung organoids (Figure 5D). Although we were unable to assess sex differences using human lung organoids *ex vivo*, these findings suggest the potential translational value of rACE2 against the SARS-CoV-2 Delta variant.

DISCUSSION

In this study, we found that female transgenic mice expressing K18-hACE2 were less vulnerable to the adverse effects of SARS-CoV-2 infection compared to male mice, aligning with previous clinical data indicating that males with COVID-19 have worse outcomes than females.[1–3] Our results suggest that biological modulations linked to sex hormones can regulate ACE2 expression and RAS, potentially making female mice more resistant to SARS-CoV-2. Additionally, we showed that inhaling rACE2 two days after SARS-CoV-2 infection effectively reduced lung damage in male mice through both neutralizing the virus and modulating cellular ACE2 levels and ERα-associated pathways. Finally, we found that treatment with rACE2 alleviated viral replication and harmful effects in human lung organoids exposed to the Delta variant of SARS-CoV-2, implying the therapeutic potential of this approach.

The mechanisms behind the sex-specific responses to SARS-CoV-2 infection are not yet fully understood. Our proteomic results showed distinct profiles in the lung microenvironment, with 6 unique proteins

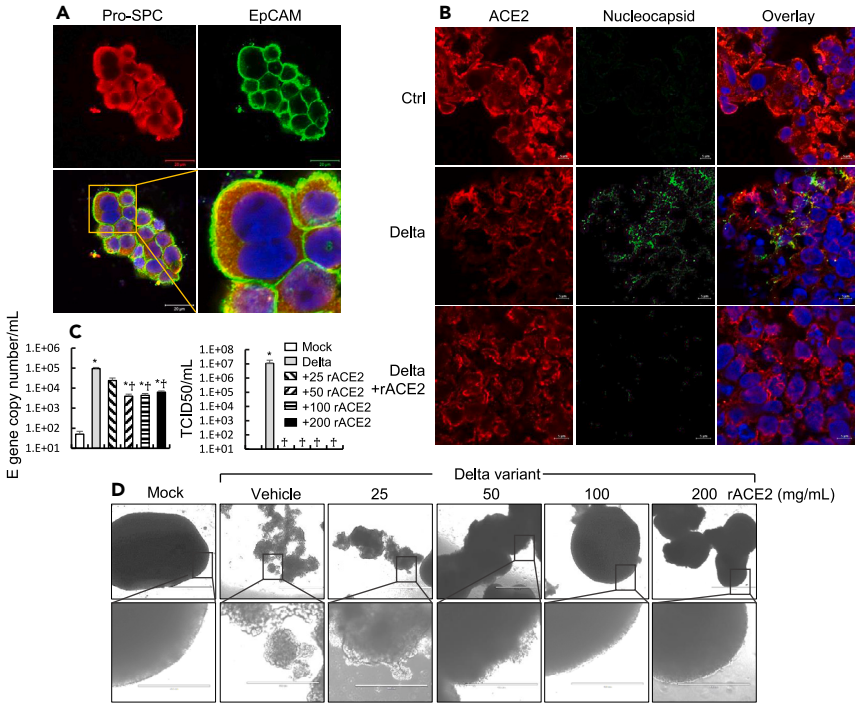

Figure 5. Treatment with rACE2 attenuates Delta variant replication and viral load and decreases cytopathic effects in human lung organoids

(A) Human lung organoids expressing pro-surfactant protein C (SPC) and epithelial cell adhesion molecule (EpCAM). Scale bars, 20 μm (main images).

(B) Representative images of human lung organoids in naive control (Ctrl, upper panel), Delta variant-challenged (middle panel), and treated with a pre-mixture of rACE2 (400 μg/mL) and Delta variant (1.8×10^7 TCID50/mL) for 30 min (lower panel). The expression of ACE2 (red) and viral nucleocapsid protein (green) were detected at 4 h post-infection. Scale bars, 5 μm. (see also Figure S4).

(C) Levels of viral envelope (E) gene RNA were assessed by qRT-PCR after treatment with various concentrations of rACE2 in human lung organoids at 3 dpi. Supernatants of the Delta variant-infected lung organoids were collected and used to infect Vero E6 cells for TCID50 assay. *$p < 0.05$ vs. Mock; ✝ $p < 0.05$ vs. Delta variant alone. Data represented in mean ± SEM.

(D) Representative images of cytopathic effects of human lung organoids in Delta variant infection and rACE2-treated groups at 3 dpi. Scale bars, 1000 μm (main images) and 400 μm (magnified). Data presented are representatives of three independent experiments.

present in female mice before and after SARS-CoV-2 infection. One example is Rho guanine nucleotide exchange factor 9 (ARHGEF9), which plays a role in regulating the immune response to viral infections, such as human cytomegalovirus (HCMV). Inhibition of ARHGEF9 has been shown to reduce immune cells' ability to respond to HCMV infection.[15] Another protein, IL-18 binding protein (IL18BP), has been shown to be crucial in controlling the immune response to viral, bacterial, and fungal infections.[16,17] RNF185 is important in regulating cellular processes relevant to host defense against infections,[18] while T cell lymphoma invasion and metastasis 1 (TIAM1) and TRPC6 play a role in regulating immune cell activation, migration, and phagocytosis, a process in which immune cells engulf and destroy pathogens in response to viral and bacterial infections.[19–21] Finally, exportin 4 (XPO4) regulates the interferon response to viral infections, a crucial component of the host defense against viruses. Some host proteins involved in antiviral responses have been shown to be substrates for XPO4-mediated export from the nucleus.[22–25] Current evidence suggests that these 6 unique proteins may play a role in regulating the host immune response to viral infection, and further research is necessary to determine if any of these deregulated proteins contribute to COVID-19 severity and if they have potential as targets for the development of new therapeutic strategies.

A correlation between ERα and ACE2 expression was observed, which could play a role in the protective effect of ERα-associated pathways in female mice recovering from SARS-CoV-2. Estrogen has been shown to interact with RAS, inhibiting renin, ACE, and angiotensin II type I receptor,[26] and enhance ACE2

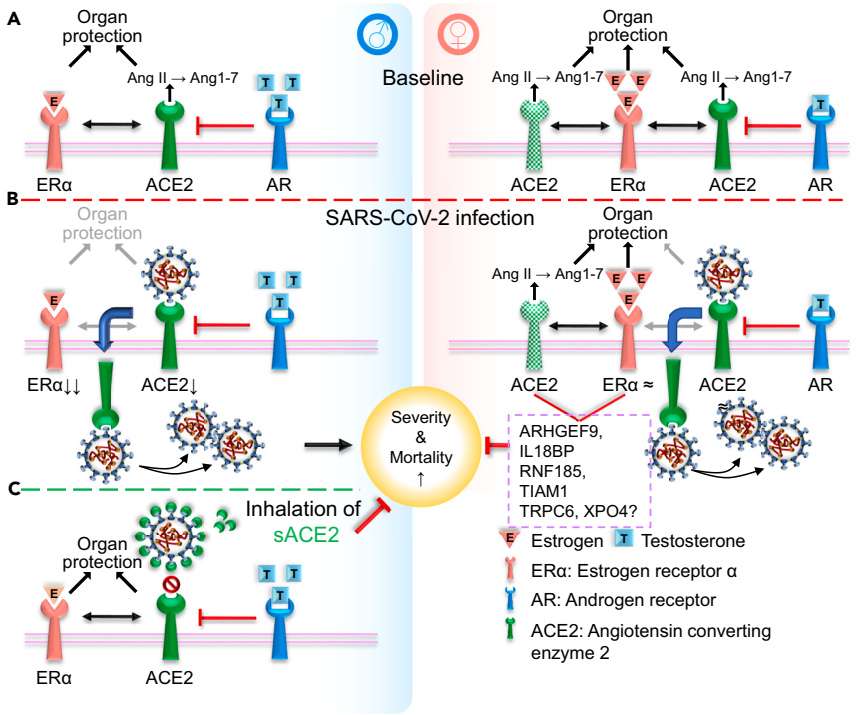

Figure 6. Proposed mechanisms underlying biological sex differences in outcomes of SARS-CoV-2 and Delta variant infections and the therapeutic potential of inhaled ACE2

(A) Under physiological conditions, ACE2 catalyzes the conversion of Ang II to Ang1-7 for organ protection. The ACE2 gene is located at X chromosome p22.2, where genes are known to escape X-inactivation,[7] contributing to phenotypic differences of ACE2 between biological sexes. Membrane expression of ACE2 can be upregulated by estrogens through estrogen receptor α (ERα),[10] which exerts anti-inflammatory properties and further enhances organ protection. In contrast, androgen receptor (AR) can cleave ACE2 and mediate pro-inflammation and tissue injury.[44].

(B) During SARS-CoV-2 infection, the virus binds to and decreases host cell surface ACE2. For a given infection, the reduction of endogenous ACE2 expression is associated with a dramatic decrease in ERα expression, resulting in loss of organ protection in males. In contrast, expression of endogenous ACE2 was sustained in females, potentially due to the extra X-linked ACE2 and well-maintained ERα expression, leading to compensatory mechanisms and persistent organ protection.

(C) Inhalation of rACE2 can restore the balance of endogenous ACE2 and ERα by blocking or attenuating SARS-CoV-2 from binding to membrane ACE2 in males.

expression through interaction with the estrogen response element in the ACE2 promoter.[10,11] Our results well fit with the recent findings demonstrating that interactions between SARS-CoV-2 spike proteins and ERα are involved in SARS-CoV-2 infection via modulation of ERα signaling and transcriptional regulation of ACE2.[27] Clinical trials are underway to examine the effects of estrogen (NCT04359329) and progesterone (NCT04365127) treatment on COVID-19 patients.

Considering the dual function of cellular ACE2, the differing severity of COVID-19 between males and females may result from multiple mechanisms, including ACE2's role in regulating the RAS system. Our hypothesis is that when SARS-CoV-2 bind to ACE2 in both males and females, the ACE2 on the second X chromosome may induce cleavage of Ang II to form Ang 1–7, providing protective effects against pulmonary edema during COVID-19 in females.[28] This advantage may be unique to females as their two X chromosomes work together to combat the virus. In contrast, men, who have only one X chromosome, lack this protective mechanism. Previous research has shown that the ACE2/ACE balance plays a role in protection against ALI.[29,30] SARS-CoV-1 infection has been reported to reduce cellular ACE2 expression in the lung and myocardium in mice.[28,31] Our findings also show a decrease in ACE2 expression in the lung after infection with SARS-CoV-2. However, this deficiency in organ protection may be less severe in females due to the presence of two X chromosomes that provide an inducible compensatory mechanism for endogenous ACE2 expression.

Recent studies have shed light on the potential involvement of testosterone levels in mediating this observed sex disparity in patients with COVID-19.[32] The findings provided by Cinislioglu et al.[33] indicate a correlation between low testosterone levels and COVID-19 severity in male patients. This prospective cohort study demonstrated lower serum testosterone levels in individuals with severe disease compared to those with mild-moderate symptoms, as well as in patients requiring intensive care compared to those who did not. These findings suggest that testosterone deficiency may contribute to the severity of COVID-19 symptoms in males. One possible explanation for the association between lower testosterone levels and disease severity could be the presence of a heightened pro-inflammatory milieu. Testosterone deficiency has been linked to increased levels of pro-inflammatory cytokines.[34] The elevated pro-inflammatory state associated with testosterone deficiency may potentially exacerbate the inflammatory response triggered by SARS-CoV-2 infection, leading to more severe disease outcomes. The association between low testosterone levels and increased COVID-19 severity in males highlights the potential impact of hormonal factors on disease outcomes. In light of these findings, the observed decrease in AR expression following SARS-CoV-2 infection further supports the importance of exploring the role of androgen signaling in mediating sex disparities in COVID-19.[35]

Our previous studies have demonstrated the efficacy of rACE2 in combating SARS-CoV-2 infection both *in vitro*[36] and in a human case report.[37] In this current study, we present a new therapy that involves delivering rACE2 via aerosol, which enhances the expression of endogenous ACE2 in the lungs. This results in a reduction of viral load and inflammation caused by SARS-CoV-2, thereby protecting the lungs from damage. To our surprise, we found that mice treated with rACE2 through nebulization showed a restored ERα/AR ratio. The exact mechanisms behind this change are still unclear, but our analysis suggests that rACE2 nebulization might restore the ERα-associated signaling proteomic profile in male mice to a pattern similar to that of female mice without treatment. Our findings highlight 16 proteins as potential targets for further investigation into how rACE2's protective effects might be achieved through the activation of ERα-related signaling pathways, in conjunction with endogenous ACE2, to fight SARS-CoV-2 infection and COVID-19.

Prior to the emergence of the Omicron variant, the Delta variant accounted for over 99% of COVID-19 cases (https://www.who.int/news/item/28-11-2021-update-on-omicron). Our study shows that treatment with rACE2 reduced the load of the Delta variant and protected human lung organoids from developing cytopathic effects. These findings are significant for several reasons. Firstly, it indicates that the ability of rACE2 to bind to the Delta variant is not compromised, allowing rACE2 to act as a decoy receptor to neutralize the Delta variant. Secondly, the protective effect of rACE2 against the Delta variant was observed in human lung organoids, which are considered advanced, complex, and reproducible *ex vivo* models for studying human lung diseases.[38]

In conclusion, this study sheds light on the differences in COVID-19 severity between males and females. Our findings indicate that the spike protein of SARS-CoV-2 reduces host cell surface ACE2 and ERα expression in males, leading to less protection for their organs. Conversely, females have sustained ACE2 expression and higher ERα levels, providing better protection for their organs. Our research suggests that inhaling rACE2 may restore ACE2 and ERα expression and serve as a decoy receptor for viral neutralization, making it a potential therapeutic approach for SARS-CoV-2 infections, including the Delta variant (Figure 6).

Limitation of the study

Further exploration is needed to understand the role of unique proteins present in female mice against SARS-CoV-2 infection and the effectiveness of rACE2 as a prophylactic and therapeutic measure against the Omicron variant. The Omicron variant is more likely to cause upper airway infections,[39–41] and it evades immune response while maintaining robust ACE2 binding.[42,43] Therefore, studying the impact of our novel aerosol administration of rACE2 on upper airway immunity is crucial and merits further research.

STAR★METHODS

Detailed methods are provided in the online version of this paper and include the following:

- KEY RESOURCES TABLE
- RESOURCE AVAILABILITY
  - Lead contact

- Materials availability
- Data and code availability
- EXPERIMENTAL MODEL AND STUDY PARTICIPANT DETAILS
  - Cell lines
  - Animal model
- METHOD DETAILS
  - Biosafety
  - SARS-CoV-2 and delta variant
  - Sex-biased responses to sars-cov-2 infection in the lung and brain in mice
  - Pharmacokinetic study of intravenous administration of rACE2 in rabbits
  - Pharmacokinetic study of nebulized recombinant ACE2 (rACE2) in healthy mice
  - Assessment of hACE2 in plasma and tissue
  - Stability test of nebulized rACE2
  - Antiviral assessment of nebulized rACE2
  - Nebulization of rACE2 in mice infected with SARS-CoV-2
  - Tissue sample processing
  - Human iPSC-derived lung organoids for SARS-CoV-2 infection
  - qRT-PCR
  - Western blotting
  - Immunohistochemistry
  - Enzyme-Linked immunosorbent assay (ELISA)
  - Proteomics analysis
- QUANTIFICATION AND STATISTICAL ANALYSIS

SUPPLEMENTAL INFORMATION

Supplemental information can be found online at https://doi.org/10.1016/j.isci.2023.107470.

ACKNOWLEDGMENTS

We sincerely thank Drs. Scott Gray-Owen and Natasha Christie for programmatic administrative and regulatory support and planning within the Combined Containment Levels 3 Facility, Temerty Faculty of Medicine, the University of Toronto. We thank Dr. Leanne Wybenga-Groot, SickKids Proteomics, Analytics, Robotics & Chemical Biology Center (SPARC) at the Peter Gilgan Center for Research and Learning (PGCRL), Hospital for Sick Children, Toronto, for providing proteomic analysis. We also thank Dr. Caterina Di Ciano-Olivera for help with image analysis.

This work was supported by the Canadian Institutes of Health Research (OV3-170344, SBC-171482, and VS.1-175560 to H. Z.). J.M.P. is funded by the Vienna Science and Technology Fund (WWTF) through project COV20-002, the Austrian Academy of Sciences and the City of Vienna and grants from the Austrian Science Fund (FWF) Wittgenstein award (Z 271-B19), the T. Von Zastrow Foundation, the Innovative Medicines Initiative 2 Joint Undertaking (JU) under grant agreement No 101005026, the Canada 150 Research Chairs Program F18-01336, and the Canadian Institutes of Health Research COVID-19 grants F20–02343 and F20-02015.

AUTHOR CONTRIBUTIONS

Conceptualization, JMP, AS, and HZ; Investigation, YO, JL, YL, BG, TT, CL, JZ, JKhateeb, JK, MJ, and GW; Writing-original draft, YO, JL, YL, and BG; Writing-review and editing, all authors; visualization, YL and HZ; supervision, ML, TM, WZ, MN, BO, AB, YWC, GW, JMP, OR, YML, SM, AS, and HZ; Equal contribution, YO and JL.

DECLARATION OF INTERESTS

GW is an employee, JP a shareholder, and AS an advisor of Apeiron Biologics AG developing soluble ACE2 as a therapy for COVID-19. The other authors declare no competing interests.

Received: April 11, 2023
Revised: June 2, 2023
Accepted: July 21, 2023
Published: July 25, 2023

REFERENCES

1. Dudley, J.P., and Lee, N.T. (2020). Disparities in Age-specific Morbidity and Mortality From SARS-CoV-2 in China and the Republic of Korea. Clin. Infect. Dis. *71*, 863–865. https://doi.org/10.1093/cid/ciaa354.

2. Peckham, H., de Gruijter, N.M., Raine, C., Radziszewska, A., Ciurtin, C., Wedderburn, L.R., Rosser, E.C., Webb, K., and Deakin, C.T. (2020). Male sex identified by global COVID-19 meta-analysis as a risk factor for death and ITU admission. Nat. Commun. *11*, 6317. https://doi.org/10.1038/s41467-020-19741-6.

3. Grasselli, G., Zangrillo, A., Zanella, A., Antonelli, M., Cabrini, L., Castelli, A., Cereda, D., Coluccello, A., Foti, G., Fumagalli, R., et al. (2020). Baseline Characteristics and Outcomes of 1591 Patients Infected With SARS-CoV-2 Admitted to ICUs of the Lombardy Region, Italy. JAMA *323*, 1574–1581. https://doi.org/10.1001/jama.2020.5394.

4. Gomez, J.M.D., Du-Fay-de-Lavallaz, J.M., Fugar, S., Sarau, A., Simmons, J.A., Clark, B., Sanghani, R.M., Aggarwal, N.T., Williams, K.A., Doukky, R., and Volgman, A.S. (2021). Sex Differences in COVID-19 Hospitalization and Mortality. J. Womens Health *30*, 646–653. https://doi.org/10.1089/jwh.2020.8948.

5. Li, Y., Jerkic, M., Slutsky, A.S., and Zhang, H. (2020). Molecular mechanisms of sex bias differences in COVID-19 mortality. Crit. Care *24*, 405. https://doi.org/10.1186/s13054-020-03118-8.

6. Zhang, H., Penninger, J.M., Li, Y., Zhong, N., and Slutsky, A.S. (2020). Angiotensin-converting enzyme 2 (ACE2) as a SARS-CoV-2 receptor: molecular mechanisms and potential therapeutic target. Intensive Care Med. *46*, 586–590. https://doi.org/10.1007/s00134-020-05985-9.

7. Carrel, L., and Willard, H.F. (2005). X-inactivation profile reveals extensive variability in X-linked gene expression in females. Nature *434*, 400–404. https://doi.org/10.1038/nature03479.

8. Talebizadeh, Z., Simon, S.D., and Butler, M.G. (2006). X chromosome gene expression in human tissues: male and female comparisons. Genomics *88*, 675–681. https://doi.org/10.1016/j.ygeno.2006.07.016.

9. Lan, J., Ge, J., Yu, J., Shan, S., Zhou, H., Fan, S., Zhang, Q., Shi, X., Wang, Q., Zhang, L., and Wang, X. (2020). Structure of the SARS-CoV-2 spike receptor-binding domain bound to the ACE2 receptor. Nature *581*, 215–220. https://doi.org/10.1038/s41586-020-2180-5.

10. Stilhano, R.S., Costa, A.J., Nishino, M.S., Shams, S., Bartolomeo, C.S., Breithaupt-Faloppa, A.C., Silva, E.A., Ramirez, A.L., Prado, C.M., and Ureshino, R.P. (2020). SARS-CoV-2 and the possible connection to ERs, ACE2, and RAGE: Focus on susceptibility factors. FASEB J *34*, 14103–14119. https://doi.org/10.1096/fj.202001394RR.

11. Wang, Y., Shoemaker, R., Thatcher, S.E., Batifoulier-Yiannikouris, F., English, V.L., and Cassis, L.A. (2015). Administration of 17beta-estradiol to ovariectomized obese female mice reverses obesity-hypertension through an ACE2-dependent mechanism. Am. J. Physiol. Endocrinol. Metab. *308*, E1066–E1075. https://doi.org/10.1152/ajpendo.00030.2015.

12. da Silva, J.S., Gabriel-Costa, D., Wang, H., Ahmad, S., Sun, X., Varagic, J., Sudo, R.T., Ferrario, C.M., Dell Italia, L.J., Sudo, G.Z., and Groban, L. (2017). Blunting of cardioprotective actions of estrogen in female rodent heart linked to altered expression of cardiac tissue chymase and ACE2. J. Renin. Angiotensin. Aldosterone. Syst. *18*, 1470320317722270. https://doi.org/10.1177/1470320317722270.

13. Banerjee, A., Nasir, J.A., Budylowski, P., Yip, L., Aftanas, P., Christie, N., Ghalami, A., Baid, K., Raphenya, A.R., Hirota, J.A., et al. (2020). Isolation, Sequence, Infectivity, and Replication Kinetics of Severe Acute Respiratory Syndrome Coronavirus 2. Emerg. Infect. Dis. *26*, 2054–2063. https://doi.org/10.3201/eid2609.201495.

14. Calfee, C.S., Ware, L.B., Eisner, M.D., Parsons, P.E., Thompson, B.T., Wickersham, N., and Matthay, M.A.; NHLBI ARDS Network (2008). Plasma receptor for advanced glycation end products and clinical outcomes in acute lung injury. Thorax *63*, 1083–1089. https://doi.org/10.1136/thx.2008.095588.

15. Ouellette, C.P., Sánchez, P.J., Xu, Z., Blankenship, D., Zeray, F., Ronchi, A., Shimamura, M., Chaussabel, D., Lee, L., Owen, K.E., et al. (2020). Blood genome expression profiles in infants with congenital cytomegalovirus infection. Nat. Commun. *11*, 3548. https://doi.org/10.1038/s41467-020-17178-5.

16. Kaser, A., Novick, D., Rubinstein, M., Siegmund, B., Enrich, B., Koch, R.O., Vogel, W., Kim, S.H., Dinarello, C.A., and Tilg, H. (2002). Interferon-alpha induces interleukin-18 binding protein in chronic hepatitis C patients. Clin. Exp. Immunol. *129*, 332–338. https://doi.org/10.1046/j.1365-2249.2002.01911.x.

17. Iannello, A., Samarani, S., Debbeche, O., Tremblay, C., Toma, E., Boulassel, M.R., Routy, J.P., and Ahmad, A. (2009). Role of interleukin-18 in the development and pathogenesis of AIDS. AIDS Rev. *11*, 115–125.

18. Wang, Q., Huang, L., Hong, Z., Lv, Z., Mao, Z., Tang, Y., Kong, X., Li, S., Cui, Y., Liu, H., et al. (2017). The E3 ubiquitin ligase RNF185 facilitates the cGAS-mediated innate immune response. PLoS Pathog. *13*, e1006264. https://doi.org/10.1371/journal.ppat.1006264.

19. Gérard, A., van der Kammen, R.A., Janssen, H., Ellenbroek, S.I., and Collard, J.G. (2009). The Rac activator Tiam1 controls efficient T-cell trafficking and route of transendothelial migration. Blood *113*, 6138–6147. https://doi.org/10.1182/blood-2008-07-167668.

20. Peotter, J.L., Phillips, J., Tong, T., Dimeo, K., Gonzalez, J.M., Jr., and Peters, D.M. (2016). Involvement of Tiam1, RhoG and ELMO2/ILK in Rac1-mediated phagocytosis in human trabecular meshwork cells. Exp. Cell Res. *347*, 301–311. https://doi.org/10.1016/j.yexcr.2016.08.009.

21. Riazanski, V., Gabdoulkhakova, A.G., Boynton, L.S., Eguchi, R.R., Deriy, L.V., Hogarth, D.K., Loaëc, N., Oumata, N., Galons, H., Brown, M.E., et al. (2015). TRPC6 channel translocation into phagosomal membrane augments phagosomal function *112*, E6486–E6495. https://doi.org/10.1073/pnas.1518966112.

22. Metwally, M., Bayoumi, A., Khan, A., Adams, L.A., Aller, R., García-Monzón, C., Arias-Loste, M.T., Bugianesi, E., Miele, L., Anna, A., et al. (2021). Copy number variation and expression of exportin-4 associates with severity of fibrosis in metabolic associated fatty liver disease. EBioMedicine *70*, 103521. https://doi.org/10.1016/j.ebiom.2021.103521.

23. Damann, N., Owsianik, G., Li, S., Poll, C., and Nilius, B. (2009). The calcium-conducting ion channel transient receptor potential canonical 6 is involved in macrophage inflammatory protein-2-induced migration of mouse neutrophils. Acta Physiol. *195*, 3–11. https://doi.org/10.1111/j.1748-1716.2008.01918.x.

24. Finney-Hayward, T.K., Popa, M.O., Bahra, P., Li, S., Poll, C.T., Gosling, M., Nicholson, A.G., Russell, R.E.K., Kon, O.M., Jarai, G., et al. (2010). Expression of transient receptor potential C6 channels in human lung macrophages. Am. J. Respir. Cell Mol. Biol. *43*, 296–304. https://doi.org/10.1165/rcmb.2008-0373OC.

25. Zhang, S., Wang, H., Liu, Y., Yang, W., Liu, J., Han, Y., Liu, Y., Liu, F., Sun, L., and Xiao, L. (2020). Tacrolimus ameliorates tubulointerstitial inflammation in diabetic nephropathy via inhibiting the NFATc1/TRPC6 pathway. J. Cell Mol. Med. *24*, 9810–9824. https://doi.org/10.1111/jcmm.15562.

26. Gallagher, P.E., Li, P., Lenhart, J.R., Chappell, M.C., and Brosnihan, K.B. (1999). Estrogen regulation of angiotensin-converting enzyme mRNA. Hypertension *33*, 323–328. https://doi.org/10.1161/01.hyp.33.1.323.

27. Solis, O., Beccari, A.R., Iaconis, D., Talarico, C., Ruiz-Bedoya, C.A., Nwachukwu, J.C., Cimini, A., Castelli, V., Bertini, R., Montopoli, M., et al. (2022). The SARS-CoV-2 spike protein binds and modulates estrogen receptors. Sci. Adv. *8*, eadd4150. https://doi.org/10.1126/sciadv.add4150.

28. Kuba, K., Imai, Y., Rao, S., Gao, H., Guo, F., Guan, B., Huan, Y., Yang, P., Zhang, Y., Deng, W., et al. (2005). A crucial role of angiotensin converting enzyme 2 (ACE2) in SARS coronavirus-induced lung injury. Nat. Med. *11*, 875–879. https://doi.org/10.1038/nm1267.

29. Imai, Y., Kuba, K., Rao, S., Huan, Y., Guo, F., Guan, B., Yang, P., Sarao, R., Wada, T., Leong-Poi, H., et al. (2005). Angiotensin-converting enzyme 2 protects from severe

acute lung failure. Nature *436*, 112–116. https://doi.org/10.1038/nature03712.

30. Zhang, R., Pan, Y., Fanelli, V., Wu, S., Luo, A.A., Islam, D., Han, B., Mao, P., Ghazarian, M., Zeng, W., et al. (2015). Mechanical Stress and the Induction of Lung Fibrosis via the Midkine Signaling Pathway. Am. J. Respir. Crit. Care Med. *192*, 315–323. https://doi.org/10.1164/rccm.201412-2326OC.

31. Oudit, G.Y., Kassiri, Z., Jiang, C., Liu, P.P., Poutanen, S.M., Penninger, J.M., and Butany, J. (2009). SARS-coronavirus modulation of myocardial ACE2 expression and inflammation in patients with SARS. Eur. J. Clin. Invest. *39*, 618–625. https://doi.org/10.1111/j.1365-2362.2009.02153.x.

32. Baratchian, M., McManus, J.M., Berk, M.P., Nakamura, F., Mukhopadhyay, S., Xu, W., Erzurum, S., Drazba, J., Peterson, J., Klein, E.A., et al. (2021). Androgen regulation of pulmonary AR, TMPRSS2 and ACE2 with implications for sex-discordant COVID-19 outcomes. Sci. Rep. *11*, 11130. https://doi.org/10.1038/s41598-021-90491-1.

33. Cinislioglu, A.E., Cinislioglu, N., Demirdogen, S.O., Sam, E., Akkas, F., Altay, M.S., Utlu, M., Sen, I.A., Yildirim, F., Kartal, S., et al. (2022). The relationship of serum testosterone levels with the clinical course and prognosis of COVID-19 disease in male patients: A prospective study. Andrology *10*, 24–33. https://doi.org/10.1111/andr.13081.

34. Mohamad, N.V., Wong, S.K., Wan Hasan, W.N., Jolly, J.J., Nur-Farhana, M.F., Ima-Nirwana, S., and Chin, K.Y. (2019). The relationship between circulating testosterone and inflammatory cytokines in men. Aging Male *22*, 129–140. https://doi.org/10.1080/13685538.2018.1482487.

35. Giovanelli, L., and Quinton, R. (2021). Androgenicity-not serum testosterone-correlates best with COVID-19 outcome in European males. EBioMedicine *66*, 103286. https://doi.org/10.1016/j.ebiom.2021.103286.

36. Monteil, V., Kwon, H., Prado, P., Hagelkrüys, A., Wimmer, R.A., Stahl, M., Leopoldi, A., Garreta, E., Hurtado Del Pozo, C., Prosper, F., et al. (2020). Inhibition of SARS-CoV-2 Infections in Engineered Human Tissues Using Clinical-Grade Soluble Human ACE2. Cell *181*, 905–913.e7. https://doi.org/10.1016/j.cell.2020.04.004.

37. Zoufaly, A., Poglitsch, M., Aberle, J.H., Hoepler, W., Seitz, T., Traugott, M., Grieb, A., Pawelka, E., Laferl, H., Wenisch, C., et al. (2020). Human recombinant soluble ACE2 in severe COVID-19. Lancet Respir. Med. *8*, 1154–1158. https://doi.org/10.1016/S2213-2600(20)30418-5.

38. McCracken, K.W., Catá, E.M., Crawford, C.M., Sinagoga, K.L., Schumacher, M., Rockich, B.E., Tsai, Y.H., Mayhew, C.N., Spence, J.R., Zavros, Y., and Wells, J.M. (2014). Modelling human development and disease in pluripotent stem-cell-derived gastric organoids. Nature *516*, 400–404. https://doi.org/10.1038/nature13863.

39. Martin, B., DeWitt, P.E., Russell, S., Sanchez-Pinto, L.N., Haendel, M.A., Moffitt, R., and Bennett, T.D. (2022). Acute Upper Airway Disease in Children With the Omicron (B.1.1.529) Variant of SARS-CoV-2-A Report From the US National COVID Cohort Collaborative. JAMA Pediatr. *176*, 819–821. https://doi.org/10.1001/jamapediatrics.2022.1110.

40. McMahan, K., Giffin, V., Tostanoski, L.H., Chung, B., Siamatu, M., Suthar, M.S., Halfmann, P., Kawaoka, Y., Piedra-Mora, C., Jain, N., et al. (2022). Reduced pathogenicity of the SARS-CoV-2 omicron variant in hamsters. Med (N Y) *3*, 262–268.e4. https://doi.org/10.1016/j.medj.2022.03.004.

41. Sheward, D.J., Kim, C., Fischbach, J., Muschiol, S., Ehling, R.A., Björkström, N.K., Karlsson Hedestam, G.B., Reddy, S.T., Albert, J., Peacock, T.P., and Murrell, B. (2022). Evasion of neutralising antibodies by omicron sublineage BA.2.75. Lancet Infect. Dis. *22*, 1421–1422. https://doi.org/10.1016/S1473-3099(22)00524-2.

42. Hoffmann, M., Zhang, L., and Pöhlmann, S. (2022). Omicron: Master of immune evasion maintains robust ACE2 binding. Signal Transduct. Target. Ther. *7*, 118. https://doi.org/10.1038/s41392-022-00965-5.

43. Mannar, D., Saville, J.W., Zhu, X., Srivastava, S.S., Berezuk, A.M., Tuttle, K.S., Marquez, A.C., Sekirov, I., and Subramaniam, S. (2022). SARS-CoV-2 Omicron variant: Antibody evasion and cryo-EM structure of spike protein-ACE2 complex. Science *375*, 760–764. https://doi.org/10.1126/science.abn7760.

44. Deng, Q., Rasool, R.U., Russell, R.M., Natesan, R., and Asangani, I.A. (2021). Targeting androgen regulation of TMPRSS2 and ACE2 as a therapeutic strategy to combat COVID-19. iScience *24*, 102254. https://doi.org/10.1016/j.isci.2021.102254.

45. Chen, Y.W., Huang, S.X., de Carvalho, A.L.R.T., Ho, S.H., Islam, M.N., Volpi, S., Notarangelo, L.D., Ciancanelli, M., Casanova, J.L., Bhattacharya, J., et al. (2017). A three-dimensional model of human lung development and disease from pluripotent stem cells. Nat. Cell Biol. *19*, 542–549. https://doi.org/10.1038/ncb3510.

46. Alexander, D.J., Collins, C.J., Coombs, D.W., Gilkison, I.S., Hardy, C.J., Healey, G., Karantabias, G., Johnson, N., Karlsson, A., Kilgour, J.D., and McDonald, P. (2008). Association of Inhalation Toxicologists (AIT) working party recommendation for standard delivered dose calculation and expression in non-clinical aerosol inhalation toxicology studies with pharmaceuticals. Inhal. Toxicol. *20*, 1179–1189. https://doi.org/10.1080/08958370802207318.

47. Haschke, M., Schuster, M., Poglitsch, M., Loibner, H., Salzberg, M., Bruggisser, M., Penninger, J., and Krähenbühl, S. (2013). Pharmacokinetics and pharmacodynamics of recombinant human angiotensin-converting enzyme 2 in healthy human subjects. Clin. Pharmacokinet. *52*, 783–792. https://doi.org/10.1007/s40262-013-0072-7.

48. Motulsky, H.J., and Brown, R.E. (2006). Detecting outliers when fitting data with nonlinear regression: a new method based on robust nonlinear regression and the false discovery rate. BMC Bioinformatics *7*, 123. https://doi.org/10.1186/1471-2105-7-123.

49. Krieger, J.R., Wybenga-Groot, L.E., Tong, J., Bache, N., Tsao, M.S., and Moran, M.F. (2019). Evosep one enables robust deep proteome coverage using tandem mass tags while significantly reducing instrument time. J. Proteome Res. *18*, 2346–2353. https://doi.org/10.1021/acs.jproteome.9b00082.

STAR★METHODS

KEY RESOURCES TABLE

REAGENT or RESOURCE	SOURCE	IDENTIFIER
Antibodies		
Nucleocapsid	Invitrogen	Cat# MA5-36251; RRID: AB_2890565
hACE2	Abcam	Cat#108252; RRID: AB_10864415
GAPDH	Cell Signalling	Cat# 5174; RRID: AB_10622025
S100B	Abcam	Cat# AB52642; RRID: AB_882426
AR	Abcam	Cat# AB108341; RRID: AB_10865716
RAGE	Abcam	Cat# AB37647; RRID: AB_777613
ERα	Abcam	Cat# AB32063; RRID: AB_732249
TMPRSS2	Abcam	Cat# AB92323; RRID: AB_10585592
B-actin	Sigma	Cat# A5316; RRID: AB_476743
Pro-SPC	Millipore Sigma	Cat# AB3786; RRID: AB_91588
EPCAM	Biolegend	Cat# 324202; RRID: AB_756076
ACE2	Abcam	Cat# AB15348; RRID: AB_301861
Nucleocapsid	Invitrogen Abcam	Cat# MA5-36251; RRID: AB_2890565 (For lung tissue) Cat# 273434; RRID: AB_2893371 (For lung organoid)
Alexa Fluor® 594 AffiniPure Goat Anti-Rabbit IgG (H+L)	Jackson Immunolabs	Cat# 111-585-144; RRID: AB_2307325
Alexa Fluor® 488 AffiniPure Goat Anti-Mouse IgG (H+L)	Jackson Immunolabs	Cat# 111-545-003; RRID: AB_2338059
DAPI	Sigma	D9542; RRID: AB_301792
Bacterial and virus strains		
SARS-CoV-2 SB2	Isolated from patient	N/A
SARS-CoV-2 Delta	Isolated from patient	N/A
Chemicals, peptides, and recombinant proteins		
Clarity and Clarity Max ECL Western Blotting Substrates	Bio-Rad	Cat# 1705062
1% Triton X-100	Boston Bio Products	Cat# BP-117
Critical commercial assays		
QiaAmp Viral RNA Mini kit	Qiagen	Cat# 52906
RNeasy mini kit	Qiagen	Cat# 74106
Luna Universal one-step rt-qpcr kit	NEB	Cat# E3005L
RAGE ELISA kit	Abcam	Cat# AB190807
17β estradiol ELISA kit	Abcam	Cat# AB108667
hACE2 ELISA kit	Abcam	Cat# AB235649
Mouse estrogen receptor alpha ELISA kit	Abbexa	Cat# abx254060
Deposited data		
Datasets	this paper	https://doi.org/10.1093/nar/gkz1019, PMID:31691833 with the identifier MTBLS8177 https://www.ebi.ac.uk/metabolights/MTBLS8177
Biological samples		
Vero E6 cells	ATCC	CRL-1586
iPSC-derived lung organoids		

(*Continued on next page*)

Continued

REAGENT or RESOURCE	SOURCE	IDENTIFIER
Oligonucleotides		
2019-nCoV Charité/Berlin Primers E gene E_Sarbeco_F1 Forward Primer: CAGGTACGTT AATAGTTAATAGCGT E_Sarbeco_R2 Reverse Primer: ATATTGCAGC AGTACGCACACA	IDT	10006888 10006890
Human RNASE P Forward Primer : AGA TTT GGA CCT GCG AGC G Human RNASE P Reverse Primer : GAG CGG CTG TCT CCA CAA GT	IDT	10006836 10006837
Mouse IL-6 Forward Primer : GACAAAGCCAGAGTCCTTGAGAGAG Mouse IL-6 Reverse Primer : CTAGGTTTGCCGAGTAGATCTC	IDT	299007077 299007078
Recombinant DNA		
2019-nCoV Charité/Berlin RUO Plasmid Controls	IDT	10006896
Software and algorithms		
Microsoft Excel	Microsoft	http://www.microsoft.com
Image Lab Software Version 6.1	Bio-Rad	http://www.bio-rad.com
GraphPad Prism 8 (GraphPad)	Motulsky and Brown, 2006[48]	https://www.graphpad.com
Orange3 (ver. 3.29.3)	University of Ljubljana	https://www.orangedatamining.com/
String (ver 11.5)	String Consortium	https://www.string-db.org
UniProt	UniProt Consortium	https://www.uniprot.org

RESOURCE AVAILABILITY

Lead contact

Further information and requests for resources and reagents should be directed to and will be fulfilled by the corresponding author, Dr. Haibo Zhang (haibo.zhang@unityhealth.to).

Materials availability

This study did not generate new unique reagents. Primers and reagents used were provided in key resources table, and available upon request to the corresponding author.

Data and code availability

- All original proteomics data have been deposited at in EMBL-EBI MetaboLights database and are publicly available as of the date of publication. DOI is listed in the key resources table.
- This paper does not report original code. Any additional information required to reanalyze the data reported in this paper is available from the lead contact (haibo.zhang@unithyhealth.to) upon request.

EXPERIMENTAL MODEL AND STUDY PARTICIPANT DETAILS

Cell lines

We maintained Vero E6 cells, African green monkey cells, from the American Type Culture Collection (ATCC) in Dulbecco's modified Eagle medium (DMEM) supplemented with 10% fetal bovine serum (Sigma-Aldrich) and 1× l-glutamine and penicillin/streptomycin (Pen/Strep; Corning). All cells were incubated at 37°C with 5% CO2.

To generate human lung organoids, a stepwise directed differentiation protocol was used with human induced pluripotent stem cells (iPSCs) (HDF-mRNA) provided by Drs. Snoeck and Chen.[45] The iPSCs

were differentiated into definitive endoderm, lung progenitor cells, and mature lung organoids, which were used for the study.

Animal model

In the study, 8-10-week-old male and female K18-hACE2 [B6.Cg-Tg (K18-ACE2) 2Prlmm/J] mice], weighed 20 to 35g, purchased from the Jackson Laboratory were utilized for the animal experiments described. The study protocols described in this study were approved by the Animal Care and Use Committee (#958) at St. Michael's Hospital, the Environmental Health Service (178-Z08-2V), and the Division of Comparative Medicine (#20012664) at the University of Toronto. All mice were housed in groups, given free access to standard rodent diet and water and were randomly assigned to experimental groups.

METHOD DETAILS

Biosafety

All work involving live SARS-CoV-2 was performed in the Combined Containment Level 3 Unit (C-CL3 Unit) of the Temerty Faculty of Medicine at the University of Toronto in accordance with institutional biosafety requirements. Personnel conducting the experiment received containment level 3 training.

SARS-CoV-2 and delta variant

We used SARS-CoV-2 strain SB2,[13] previously described by our group, for this study. The delta variant (B.1.617.2) was also included, and the sequences in the stock showed furin cleavage site and furin cleavage site-proximal mutations in the spike protein. We found that these deletions attenuated the virus in hamsters (data not shown) and enhanced viral replication kinetics in VeroE6 cells.

Sex-biased responses to sars-cov-2 infection in the lung and brain in mice

In a pilot study, male wild-type and K18-hACE2 [B6.Cg-Tg (K18-ACE2) 2Prlmm/J] mice aged 8–10 weeks old were intranasally inoculated with SARS-CoV-2 strain SB2[13] at a dosage of 2×10^5 or 4×10^5 tissue culture infectious dose (TCID50) in 50 μL per mouse. We observed that the mice lost weight. This dose of SARS-CoV-2 strain SB2 was used for subsequent studies in both male and female mice.

Pharmacokinetic study of intravenous administration of rACE2 in rabbits

In this study, we investigated the pharmacokinetics of intravenously administered rACE2 in New Zealand white rabbits. A total of 12 rabbits, comprising 6 males and 6 females, with an average weight of 3.0 ± 0.1 kg were randomly divided into three groups. Group 1 received lung injury alone, Group 2 received non-lung injury with rACE2, and Group 3 received lung injury with rACE2 (Apeiron Biologics, Vienne, Austria).

To induce lung injury, intratracheal HCl (pH 1.1, 1.2 mL/kg) was administered followed by injurious ventilation for 2 h (plateau pressure 25 ± 1 cmH_2O) and high tidal volume ventilation for 4 h (Vt 10.4 ± 0.2 mL/kg) reaching P/F 150 ± 35 at the end of the experiment. The non-lung injured group was ventilated with low tidal volume (Vt 5.8 ± 0.1 mL/kg) for 6 h. IV rACE2 (0.4 mg/kg) was administered at the onset of mechanical ventilation. Plasma samples were collected hourly, and blood and lung were collected for human ACE2 measurement. To remove blood from the lung circulation, the lung was perfused with 70 mL/kg of PBS during exsanguination, and all samples were immediately stored at −80°C until further analysis.

Pharmacokinetic study of nebulized recombinant ACE2 (rACE2) in healthy mice

For nebulization, a nebulizer (Aerogen pro, Aerogen, Ireland), oxygen supply with a flow meter (VFB-92D-SSV, Dwyer, USA), and a 3 L plastic chamber were used. A high-efficiency particulate air filter (HEPA) grade heat moisture exchange filter (Adult HEPA hydrophobic bacterial/viral filter, GE Healthcare, USA) was attached to the exhaust port of the plastic chamber to contain the mist during nebulization. The delivered dose (DD) of the rACE2 was calculated using the formula developed by the Association of Inhalation Toxicologists[46]: DD (mg/kg) = [C(mg/L) x MV (L/min) x exposure time (min)]/BW. Here, C represents the concentration of srhACE2 in the mist, MV represents the minute ventilation of the rabbit, and BW represents the body weight of the rabbit. The bias flow was adjusted from 0.5 to 2.5 L/min.

Using the indicated nebulization setting, we nebulized 4.4 mL of 2% Evans blue or PBS for 15 min. After the rabbits were euthanized, lung tissue was collected, and the lung was perfused with 2 mL of PBS.

Male K18-hACE2 mice aged 8–10 weeks received soluble human recombinant ACE2 (rACE2, Apeiron Biologics, Vienna, Austria) either by intravenous injection (0.4 mg/kg) or nebulization (DD 12 mg/kg). Mice in both groups were euthanized by intraperitoneal injection of ketamine hydrochloride (200 mg/kg) and xylazine (20 mg/kg) at 2, 8, and 24 h after rACE2 administration. Blood was collected during exsanguination by cardiac puncture, and the lung was collected after perfusion with 2 mL of PBS from the right ventricle.

Assessment of hACE2 in plasma and tissue

The hACE2 concentration in both rabbit and mouse plasma and lung tissue of mice was measured by hACE2 ELISA (#ab235649: Abcam, UK) following the manufacturer's instructions. The concentration of ACE2 in rabbit lung tissue was evaluated by quantifying enzymatic activity using MCA-Ala-Pro-Lys(DNP) as a substrate.[47]

Stability test of nebulized rACE2

A total of 5.7 mg of rACE2 was distributed into a chamber through a nebulizer connected to a gas blender at a bias flow rate of 0.5 L/min at room temperature for 15 min, which is the setting used in mice. The condensation fluid in the chamber was collected for protein assay, and the size (molecular weight) and quantity of rACE2 were evaluated by sodium dodecyl sulfate-polyacrylamide gel electrophoresis (SDS-PAGE). The functional test of the condensation fluid was done by comparing its ability to block SARS-CoV-2 entry into Vero-E6 cells between pre-nebulized rACE2 and condensation fluid for viral RNA analysis.

Antiviral assessment of nebulized rACE2

The functional test of the condensation fluid was done by comparing its ability to block SARS-CoV-2 entry into Vero-E6 cells between pre-nebulized rACE2 and condensation fluid. A total of 5×10^4 Vero-E6 cells were seeded per well in a 48-well culture plate in DMEM containing 10% FBS 24 h before infection with SARS-CoV-2 or with mixes containing SARS-CoV-2 + rACE2. The stocked rACE2 and condensation fluid containing nebulized rACE2 at indicated concentrations were mixed with SARS-CoV-2 at MOI 2.0 in a final volume of 100 μL per well in DMEM (0% FBS) for 30 min on ice and then added to Vero-E6 cells (the inoculum remained unremoved). At 15 h post-infection, the supernatants were removed, and the cells were washed three times with PBS and then lysed using Buffer AVL (QiaAmp Viral kit, Qiagen) for RNA extraction for viral envelope (E) gene target assay by qRT-PCR.

Nebulization of rACE2 in mice infected with SARS-CoV-2

A group of 8-10-week-old mice were intranasally administered SARS-CoV-2 at a dose of 4×10^5 TCID50/50 μl/mouse while under general anesthesia (Isoflurane 3.5%). The experimental group received nebulized rACE2 at a dose of 1.2 or 12 mg/kg from 2 dpi until the day before sacrifice. The control group received PBS nebulization from 2 dpi until the day before sacrifice. The mice were monitored daily for body weight and were euthanized on 7 dpi under anesthesia by 3–5% isoflurane.

After euthanasia, the organs were collected, and the lung was perfused with 2 mL of PBS. The right lung and brain were minced, and each organ was divided into three tubes: 1% Triton X- with 0.01% protease inhibitor (Thermo Scientific) for protein extraction, RNA protect (Qiagen) for RNA extraction, and DMEM +1× l-glutamine and penicillin/streptomycin (Pen/Strep; Corning) for TCID50. The heart, liver, right kidney, spleen, and ileum were collected in RNA protect for RNA extraction. The left lung was inflated with 20 cmH_2O of 10% formalin and fixed in 10% formalin for 72 h for histology analysis.

Tissue sample processing

Oropharyngeal swabs were taken using fine tip Specimen collection swabs (TYPENEX Medical cat #SW0102) were placed in 500 μL of PBS and stored at −80°C until later use. Viral RNA was then isolated from the swab using the QIAamp Viral RNA Mini kit (Qiagen), as per the manufacturer's instructions.

All tissues collected for protein extraction, RNA extraction, and TCID50 assay were homogenized using a bead mill homogenizer (Bead Ruptor4, OMNI). Homogenates for protein extraction were centrifuged for 15 min at 13,000 rpm at 4°C, and the proteins in the supernatant were collected and stored at −80°C for further analysis. For RNA extraction, total RNA from the homogenate was extracted using the RNeasy Plus mini kit (Qiagen) according to the manufacturer's instructions and stored at −80°C until further analysis. For TCID50 assay, the homogenate was centrifuged for 5 min at 1500 g at 4°C, and the supernatant was

collected and used for TCID50 assay. The virus titers (50% tissue culture infectious dose [TCID50]/mL) were determined from the supernatant using the Spearman and Karber method.

Human iPSC-derived lung organoids for SARS-CoV-2 infection

For SARS-CoV-2 virus infections in the lung organoids, variable concentrations of rACE2 were pre-mixed with the Delta variant at MOI 0.1 for 30 min on ice in maturation media containing CHIR99021, KGF, FGF10, dexamethasone, IBMX, cAMP, L-ascorbic acid, and monothioglycerol (MTG) in serum-free differentiation media. The lung organoids were infected with the Delta variant at MOI 0.1 or the rACE2 and Delta mixture in maturation media, in a volume of 0.5 mL per well of a 24-well ultra-low attachment plate for 1 h. One-hour post-infection, the organoids were washed three times with PBS and kept in 1 mL of corresponding medium for 3 days. On day 3 post-infection (dpi), supernatants were recovered, and organoids were washed three times with PBS before being lysed with buffer RLT from RNeasy Plus mini kit (Qiagen). Cells were recovered 72 h post-infection (hpi), pooled (5 lung organoids per condition), and the level of infection was determined by viral RNA detection using qRT-PCR. Samples were then analyzed for the presence of viral RNA by qRT-PCR, and 35 μL of each supernatant was used for TCID50 assay in 96-well plates.

For immunofluorescence, lung organoids were infected with the Delta variant at 1.8 × 10^7 TCID50/mL or rACE2 (400 μg/mL) and Delta mixture in a volume of 0.5 mL per well of a 24-well ultra-low attachment plate for 4 h. The organoids were then washed three times with PBS and fixed with 4% paraformaldehyde for 1 h at room temperature. Expression of ACE2 (red, Alexa 594, R&D) and viral nucleocapsid protein (green, Alexa 488, Abcam) were detected in human lung organoids at 4 hpi under z stack scanning.

qRT-PCR

Total RNA samples were prepared from lung tissues/organoids using the RNeasy Plus mini kit (Qiagen) according to the manufacturer's instructions. To quantify viral replication, measured by the accumulation of subgenomic E transcripts, one-step quantitative real-time PCR was performed using the Luna Universal qPCR Master Mix (New England Biolabs) with primers specific to SARS-CoV-2 E-gene following guidelines by the World Health Organization. Quantitative real-time PCR reactions were performed on an Applied Biosystems Quant Studio 7 Flex Real-Time PCR System. The cycling conditions were 1 cycle of denaturation at 60°C for 10 min, then 95°C for 2 min, followed by 39 amplification cycles at 95°C for 10 s and 60°C for 15 s. For IL-6 mRNA, the delta-delta-cycle threshold (ΔΔCT) was determined relative to Gapdh and mock-infected/treated samples. Analysis was performed using Quant Studio Real-Time PCR Software. The sequences of primers are provided in key resources table.

Western blotting

Proteins were extracted from cells using TPER lysis buffer (Thermofisher), supplemented with 1X Complete Protease Inhibitor Cocktail (Roche) and 1X Triton X-100 (BioShop), and removed from the BSL-3 facility. The total protein concentration of the tissue lysates was measured using the Bio-Rad assay according to the manufacturer's instructions. Samples were analyzed by SDS-polyacrylamide gel electrophoresis and transferred to a 0.2 μm polyvinylidene fluoride membrane. Primary antibodies, as provided in key resources table, were used to detect proteins overnight at 4°C, followed by incubation with HRP-conjugated secondary antibodies for 1 h at 25°C. The membranes were visualized using Clarity and Clarity Max ECL Western Blotting Substrates (Bio-Rad) and detected by a Bio-Rad ChemiDoc imaging system. Densitometry was performed using ImageLab software.

Immunohistochemistry

Lung tissue from mice was histologically analyzed on paraffin-embedded sections. The tissues were fixed in 10% buffered formalin for 72 h, transferred to 70% ethanol, processed and embedded in paraffin. Adjacent sections (5 μm) were stained with haematoxylin and eosin for comparison. The lung injury score was assessed on a scale of 0–4 for the following criteria: 1) neutrophil numbers in the alveolar space, 2) alveolar septal thickening, 3) number of hyaline membranes, 4) alveolar hemorrhage, and 5) cellular hyperplasia. To fix the lung organoids, they were incubated in 4% paraformaldehyde for 1 h, followed by transfer to 15% sucrose for 24 h and then 30% sucrose for 24 h, and finally snap-frozen in O.C.T. (Sakura Finetek). Cryosectioned lung organoids were permeabilized in 0.3% Triton X-100 for 15 min. For immunofluorescence, lung organoids or deparaffinized mice lung tissue sections were immunostained with primary antibodies overnight at 4°C and secondary antibodies for 1 h at room temperature. The primary and secondary antibodies

used are listed in key resources table. Nuclei were counterstained with DAPI, and immunostained sections were viewed under a ZEISS LSM700 confocal microscopy system. The figures were processed using Zen 3.3 (blue edition).

Enzyme-Linked immunosorbent assay (ELISA)

Blood was collected via cardiac puncture from 8- to 10-week-old k18-hACE2 mice that received SARS-CoV-2 of 4 × 10^5 TCID50/50mL/mouse via intranasal administration under general anesthesia (3.5% isoflurane). The animals were nebulized with rACE2 (deliver dose 12 mg/kg) from 2dpi until the day before sacrifice. The control group received PBS nebulization from 2dpi until the day of sacrifice. Mice were euthanized on 6 or 7 dpi under anesthesia by 3–5% isoflurane and in tubes containing heparin as an anticoagulant. Blood was immediately centrifuged at 1,500 × g for 10 min at 4°C, and the resulting supernatant (plasma) was collected. The RAGE concentration was measured using an ELISA kit (Abcam, ab190807).

Lung tissue homogenates were centrifuged for 15 min at 13,000 rpm 4°C, and the collected supernatants were used to measure the concentration of 17β estradiol (Abcam, ab108667), hACE2 (Abcam, ab235649), and Estrogen receptor α (Abbexa Ltd, abx254060) using ELISA kits according to manufacturer's instructions.

Proteomics analysis

The liquid chromatography-tandem Mass spectrometry (LC/MS/MS) analysis was conducted by the SPARC BioCentre (Hospital for Sick Children, Toronto) using the Thermo Scientific Orbitrap Fusion Lumos Tribrid mass spectrometer (Thermo Scientific) following a previously described analysis method.[49] Briefly, 100 μg of proteins from each animal was lyophilized and trypsin digested to generate peptides prior to chromatographic separation and spectrometric analysis. The LC/MS/MS output peptide sequences were matched against the Uniport-mouse database using Proteome Discoverer 2.5.0.400 to make protein identifications. In total, 7,010 and 8,290 protein identifications were made in brain and lung samples, respectively. There were 1,080 protein identifications not detected in brain samples and 1,388 in lung samples. 5,930 protein identifications in brain samples and 6,902 protein identifications in lung samples were analyzed using R program. For each comparison, a non-paired t-test was performed, and the fold change of scaled abundances was calculated. Proteins with a p value ≤ 0.05 and fold change ≥ 2 (fold change ≥ 1 was used for the Male Infection Group vs. Male Therapeutic Group) were considered significant changed proteins shown as a Volcano Plot. The significantly changed proteins were grouped by biological process into 14 groups, and these groups were represented as pie charts. The scaled abundances of the proteins were then input to Orange3 (ver. 3.29.3) to generate heatmaps. Lung proteins with more than 2× up-regulation, along with RAS-related proteins and estrogen receptors (Esr1, Esr2, Gper1), were uploaded to String (ver. 11.5, https://string-db.org/) for functional clustering analysis. Proteins were clustered using k-means clustering. Additionally, data analysis was conducted using GraphPad Prism 8 (GraphPad). Statistical significance was determined by Student's t-test for the proteomic analysis.

QUANTIFICATION AND STATISTICAL ANALYSIS

Data that passed the Shapiro-Wilk normality test (ELISA, qRT-PCR, and densitometry) were analyzed using ANOVA followed by Tukey's test. Non-normal data such as lung injury score was analyzed by Kruskal-Wallis test followed by Dunn's test. For comparisons between sexes when treatments were undertaken, repeated measures of ANOVA followed by the non-parametric Friedman test were used.

To explore the correlation of protein concentrations, linear regression with robust curve fit and Pearson coefficient test were applied. Data are reported as mean ± SEM, and a p value <0.05 was considered to be statistically significant.